

Study of Absorption from Intensity Modulation and Demodulation of an Ultra-Short Pulse Laser in High Magnetic Field from Acousto-Optic Strain Dependent High Dielectric Constant Diffusive Ferroelectric Semiconductor Plasma

¹Shivani saxena, ²Sanjay Dixit, ³Sanjay Srivastava

¹Department of physics, Govt M.V. M College Barkatullah University, Bhopal, India

² Department of Physics, Govt.M.V.M. College Barkatullah University, Bhopal, India

³Department of Material Science & Metallurgical Engineering, Maulana Azad National Institute of Technology, Bhopal, India

Email: sxn_shvn@yahoo.co.in, sanjay_007dixit@rocketmail.com, s.srivastava.msme@gmail.com

Abstract: The two temperature models are reported to investigate the results of intensity And temperature depending upon pulse the pulse interaction .The propagation of ultra-short laser pulse depends upon the dielectric and the electron and electron collision frequency. The basic results are reported in terms of intensity and temperature profile .This results provides a better understanding of the amplitude modulation and demodulation of the high intensity laser wave incorporating the carrier heating (CH) effect in opto-acoustic semiconducting plasma. The carrier effects add a new dimension to investigate the results of ultra-laser pulse propagation in high strain dielectric material under a different different wave number regime over a wide range of cyclotron frequency .This result provides a better understanding of amplitude modulation and demodulation by incorporating by the CH effect effectively. Numerical estimation has been carried out by irradiating by the pump wave of $2.5 \times 10^{16} \text{ s}^{-1}$ with an ultra –short pulse in the strain dependent high dielectric ferroelectric material such as BaTiO_3 . Complete absorption of high intensity laser wave takes place in the wide range of cyclotron frequency, depending upon the variation of the modulation and demodulation of intensity with and without the diffusion of the carrier heating. This parameter is modified from variation of the temperature dependent conductivity of the material. The crossover is observed in temperature and intensity profile and negative intensity modulation is seen in opposite sides of the material .

Date of Submission: 11-05-2016

Date of acceptance: 18-12-2017

I. Introduction

After the invention of the laser in 1960, the nonlinear phenomena in the optical frequency range became easily accessible [1]. The theoretical framework describing the nonlinear response of matter with ultra-short laser pulses is built upon the nonlinear dependence of the constitutive relations of Maxwell's equations on the electric and magnetic fields [2–4]. This interaction has resulted from interactions between ultra-short laser pulses and matter. These unique properties of short pulse laser interaction with matter opened a wide application in plasma and atomic physics, such as surface micromachining, pulsed laser ablation, pulsed laser deposition, generation of nanoparticles. Particularly, special attention has been paid to the femtosecond laser heating of the electronic subsystem out of thermal equilibrium with the lattice interaction. When the laser pulse irradiates the surface of the target, matter is ejected and forms a cloud above the surface. The plasma electron conducts heat inward, and also removes the heat from the skin layer. The irradiated energy of the laser pulse is absorbed in a thin surface layer of the target, and developed the high temperature within the thin film without conducting the heat into the bulk material, which is suitable for fs laser pulse application as a promising light source for pulsed laser ablation (PLA) experiments. The ultra-short (typically <10 ps) laser heating of metals and its non-equilibrium energy, transport provide a way of creating much higher energy densities in condensed matter [5]. The removal of matter from the surface obtained by focusing a short ($\sim 10^{-13}$ to 10^{-8} s) laser pulse onto a surface, i.e., laser ablation, can be regarded as the final stage of a long chain of processes with localized heating through covering several length and time scales. The details of the interaction depend essentially on the types of the material, its properties, and laser parameters [6, 7]. A direct solid-to-plasma transition has also been reported in semiconductors and dielectrics with sub picosecond pulses at irradiances greater than $I_p \sim 10^{13} \text{ W/cm}^2$. Due to their short time duration very high intensity levels can be achieved with Femto second pulses. The properties of the medium propagated can be significantly changed by Ultra short pulses, which also alter the pulse itself.

For both scientific and technological applications Understanding the propagation of femtosecond light pulses is of great value. Scientists can explore physical phenomena with unprecedented time resolution; chemical reactions can be studied at the atomic level, and ultrafast changes in material properties can be measured provided by the short pulse duration. Strong nonlinear light-matter interactions, which have led to new optical phenomena, such as the formation of spatio-temporal solitons are created by higher intensity levels achieved with ultra short laser pulses [8, 9]. From the changes in the material properties much can be learned about the propagation of pulses. The time scale of the changes ranges from instantaneous to permanent. Ultrafast nonlinear index changes can be as fast as a femtosecond or last for several picoseconds. Index changes due to heating, can last for milliseconds and Plasma generated through ionization of the material has a lifetime on the order of nanoseconds. Due to melting there can also be a permanent effect on the material, such as in the case of laser ablation or permanent index changes. To visualize the propagation of femtosecond pulses several methods have been implemented. When a high dielectric material is subject to between femtosecond Laser irradiation, the refractive index of the material may become intensity dependent and a large amount of electrons generated by the infrared pulses in transparent dielectrics. Relation channels of electronic excitation in wideband material may produce intrinsic defects, leading to photo induced damages in otherwise defect free medium. These fundamentally non linear processes have stimulated substantial efforts in both the understanding of the complexity femtosecond laser interaction with dielectric and the application of the microscopic mechanism to innovative material fabrication [10]. In the simplest case the laser can deposit the energy into a material by creating electron-hole plasma through single photon absorption However for wide band gap dielectric material the cross section of such linear absorption is extremely small. Instead under femtosecond laser irradiation nonlinear processes such as multiphoton, tunnel ionization or avalanche ionization become the dominant mechanism to create free carriers inside the materials.

The conventional view of laser –material interaction with wavelength between near IR and UR, includes the transfer of electromagnetic energy to electronic excitation, followed by electron lattice interaction that converts energy into heat. However the processes of material response following intense femtosecond pulse irradiation are far more complex, particularly wide range band gap dielectrics. The efficiency of the laser energy transfer to the matter plays a central role in different physical processes and phenomena specific to laser produced plasmas. It has been shown that the energy absorption has an impact on various physical processes, including energetic particle acceleration, high harmonic generation and hard X-ray production. Absorption depends on a large number of physical conditions which can control and optimize the coupling of the laser energy [11]. Ultra short x-ray pulses are generated by these high-density plasmas with extremely sharp density gradients. The laser pulse should rise from the intensity level corresponding to the threshold of plasma formation to the peak value in a time much shorter than the time scale of plasma expansion to produce such plasma. The time-integrated spatial profile of the beam can be reconstructed and one can measure a trace left in a material after a pulse has gone through if temporal resolution is not required. For example, for pulse propagation through solids, if there is permanent damage in the material the beam profile can be inferred from the damage tracks In particular, recent studies concentrated on the dependence of laser polarization and pre plasma density profiles on these processes at ultrahigh laser intensities [12, 13]. The choice of the investigated materials, is governed by their practical applications in optical and semiconductor technologies which consequently determines the used laser wavelengths and pulse durations [14-16].

In this present article, the theoretical aspect was considered to deal with the problem of interaction with high dielectric material such as BaTiO₃ ferroelectric material. We try to investigate the effect of carrier heating (CH) on the amplitude modulation and demodulation of the high intense laser wave with small pulse of 100 fs. The highly intense beam generates the acoustic wave within BaTiO₃ (by electrostrictive coefficient) that induces the plasma in high magnetic field and acoustic phonon from the vibration of the lattice of the material. This interaction provides the strong space modulation and demodulation of the electric field and intensity at the resonance frequency of the high intense laser wave. Theses interaction can produce the modulation and demodulation of the wave effectively at the acoustic wave. These acoustic nature is also changed the temperature profile by the absorbing the high intense laser wave with ultra-short pulse.

II. Theoretical Formulation

Let us consider the two-temperature model of metal heating by a femtosecond laser pulses on metals [17-21]. The model consists of a system of heat-conduction equations for the electrons and the phonons (lattice) subsystems, where thermo physical properties depend on electron temperature T_e and electron concentration n , and the equation describing the temporal evolution of the electron concentration.

$$C_e(T_e, n) \frac{\partial T_e}{\partial t} - \frac{\partial}{\partial x} \left(k [T_e, n](x) \frac{\partial T_e}{\partial x} \right) = -\beta_{ei}(T_e, n)(x)(T_e - T_i) + Q_v(T_e, n)(x) \quad (1.1)$$

$$C_i \frac{\partial T_i}{\partial t} - \frac{\partial}{\partial x} \left(k [T_i, n](x) \frac{\partial T_e}{\partial x} \right) = -\beta_{ei}(T_e, n)(x)(T_e - T_i) \quad (1.2)$$

Where $\lambda_e, \lambda_i, C_e, C_i$ are the electron and lattice heat conductivity and heat capacity, β_{ei} – electron-ion energy transfer coefficient, q_v – the absorbed power density released in the electron subsystem. Dependence of optical and thermo-physical properties of metal [22] on the electron temperature and concentration is taken into account

for electron heat capacity: $C_e = \frac{\pi^2 k_b^2 n(z, t) T_e}{2 \varepsilon_F}$, electron heat conductivity: $k_e = \frac{v_{ee}^2 \tau_{ee} C_e}{3}$ electron-ion

energy transfer coefficient: $\beta_{ei} = \frac{C_e}{t_{ei}}$ electron velocity: $v_e = \sqrt{\frac{3k_b T}{m_e}}$, the electron mean free path:

$l_e = \frac{1}{n \sigma \sqrt{2}}$. The absorption coefficient of metals depends only on the concentration of free electrons:

$\alpha(n) = (\alpha / n_0) n$, n_0 is the initial concentration of free electrons. The Fermi energy E_F for metals is very high. For example, for copper $E_F = 7.1$ eV, for silver $E_F = 5.5$ eV. For this reason heat effects engage the electrons, whose energy lies in a narrow energy range $\approx 2k_b T$ (k_b -Boltzmann constant) near the Fermi level. The deposition of the laser pulse energy can heat the materials and raise the temperature of materials. Given that laser beam [22] is perpendicular to the surface of materials (flat surface), the temperature with respect to time t and depth x will be:

$$\Delta T(x, t) = 2(1 - R) \alpha I_0 \frac{t}{\pi k C_i \rho} \operatorname{ierfc} \frac{x}{\sqrt{2kt / \rho C_i}} \quad (1.3)$$

Where, t is the laser pulse irradiation time, R is the reflectivity, α is the absorptivity, I_0 is the spatial distribution of laser intensity, k is thermal conductivity, ρ is the density of irradiated materials. When $x > \sqrt{\frac{kt}{\rho C_i}}$ the surface temperature will be simplified as:

$$T_i(t) = T_f + 2\alpha I(t, x) \frac{\sqrt{t}}{\sqrt{\pi k C_i \rho}} \quad (1.4)$$

Using the relation between the specific heat capacity at constant pressure and the energy, the following expression for the volumetric specific heat capacity can be obtained:

$$C_V = \frac{1}{\rho V k_B T^2} \sum_{q, p} \frac{(\hbar w_{q, p}^-)^2 e^{\frac{\hbar w_{q, p}^-}{K_B T}}}{(e^{\frac{\hbar w_{q, p}^-}{K_B T}} - 1)^2} \quad (1.5)$$

The specific heat capacity can be calculated by Eq. (6.5) once the dispersion relation, $\omega = \omega_{\vec{q}}$ is established. The heat deposition rate due to laser radiation, $Q_v(T_e, n)$, is defined in the standard way by

$$Q_v(T_e, n) = \omega \operatorname{Im} [\varepsilon(t, x; \omega)] \frac{|\bar{E}_{\pm}(t, x)|^2}{8\pi} \exp\left(-\frac{(t - \tau_e)^2}{\tau_L^2}\right) \quad (1.6)$$

In this investigation the local approximation for Q_L is used by assuming the negligible effect of spatial dispersion for justification of both the solids and plasmas with electron temperature up to several hundred electron volts. To derive the electric field inside the target materials, $E(t, x)$ we solve the Maxwell wave equation for the plane monochromatic wave incident from $x = -\infty$ onto a plane target surface located at $x=0$:

$$\frac{\partial^2 E(t, x)}{\partial x^2} + \frac{\omega^2}{c^2} \varepsilon(t, x, \omega) = 0 \quad (1.7)$$

with boundary conditions $E(t, x \rightarrow \infty) = 0$ and $i \left(\frac{c}{\omega} \right) \partial_x E(t, x) \Big|_{x=0} = 2E_0(t)$ where $E_0(t)$ is the amplitude of the incident electromagnetic wave. The complex spectrum of the transmitted response $E(x, t)$ can be calculated in terms of reference spectrum $E_0(\omega)$ and the transfer function is defined by

$$\frac{E_{\pm}(x, t)}{E_0(\omega)} = \pm t_{12} t_{21} e^{iL(k-k_0)} e^{-\frac{\alpha L}{2}} \tag{1.8}$$

Where t_{12} and t_{21} are the frequency-dependent complex Fresnel transmission coefficients, L is the thickness of the sample, α is the power absorption, $k=2\pi n_r/\lambda$ and $k_0=2\pi/\lambda$ are the propagation wave vectors. For the incident electromagnetic field Gaussian laser-pulse intensity, I , profile is assumed,

$$I(t) = \frac{cE^2(t, x)}{8\pi} \exp \left[- (2 \ln 2)^2 \frac{(t - 2\tau_e)^2}{\tau_L^2} \right] \tag{1.9}$$

Where τ_e is the laser-pulse duration defined as the FWHM. The absorption (A) and reflection (R) coefficients

averaged over space (x) and time (t) are defined as follows $\langle A \rangle = \frac{\int_0^{4\pi} dt \int dx Q_L(t, x)}{4\pi}$, $\langle R \rangle = 1 - \langle A \rangle$, and $\int_0^{\infty} dt I(t)$

$$R(x, t) = \frac{(\epsilon_1 - 1)^2 + \epsilon_2^2}{(\epsilon_1 + 1)^2 + \epsilon_2^2} \tag{1.10}$$

This τ_g can be either the actual Gaussian pulse duration, or the time needed for electrons to transfer the absorbed energy to the lattice for a sub-ps laser pulse. From the Beer-Lambert law, the intensity of an electromagnetic wave inside a material falls off exponentially from the surface as:

$$I(z) = I \exp \left(- \frac{\Delta z}{\delta} \right) = \frac{cE^2(x, t)}{8\pi} \exp \left(- (2 \ln 2)^2 \frac{(t - 2\tau_e)^2}{\tau_L^2} \right) \exp \left(- \frac{\Delta z}{\delta} \right) \tan \theta \tag{1.11}$$

Where $I(z)$ is the laser beam intensity in the material, I_0 is the incident laser beam intensity at the sample surface. δ denotes optical penetration depth. The laser energy absorbed by the material change in the kinetic energy of atoms, which is realized through the scaling the velocities with factor χ , expressed as:

$$\chi = \left(1 + \frac{\Delta E_{abs}}{E_K} \right)^{1/2} \tag{1.12}$$

The intense pump beam induces the acoustic wave within the semiconductor media by the interaction between the free carrier and acoustic phonon (through material vibration). This interaction induces a strong space field that modulates/or demodulates the pump wave. Thus, by applying the electric field and induce the acoustic wave inside the semiconducting materials can produce the amplitude modulation and demodulation effects from the acoustic wave frequency. In order to obtain the magnetically induced modulation a demodulation indices can be given by solving the (1.6)

$$\vec{E}_{\pm}(x, t) = \pm E_0 \frac{2i\omega_0 \mu_0 c e u \epsilon_0 g A^2 (\omega_0^2 - \nu^2 - \omega_c^2) k_a}{m \beta [(\omega_c^2 + \nu^2 - \omega_0^2)^2 + 4\nu^2 \omega_0^2] (k_a \pm 2k)} \left[1 + \frac{D \nu k^2}{\epsilon_0 \epsilon_L \omega_p^2} \right] \exp [i(\omega_0 t - k_0 z)] \tag{1.13}$$

The frequency-dependent complex dielectric function $\epsilon(\omega)$ is determined from absorption spectrum and the refractive index is calculated from dielectric data, - i.e., $\epsilon(\omega) = (n_r + i n_i)^2$, where the imaginary part of the refractive index n_i is related to the power absorption as $n_i(\omega) = \alpha(\omega) \lambda / 4\pi$. The real and imaginary parts of

dielectric constants are determined by the equations $\epsilon_r = (n_r^2 - n_i^2) = n_r^2 - \left(\frac{\alpha \lambda}{4\pi} \right)^2$ and

$\epsilon_i = 2 n_i n_r = \alpha n_r \lambda / 2\pi$ respectively. The classical pseudoharmonic model is used to frame out the complex dielectric function of

$$\epsilon_m(\omega) = \epsilon_\infty + \frac{(\epsilon_0 - \epsilon_\infty)\omega_{TO}^2}{\omega_{TO}^2 - \omega^2 - i\gamma_{TO}\omega} \tag{1.14}$$

From the quantum mechanical approaches, the complex dielectric function ϵ_m of pure can be expressed as the product of each oscillator with four parameters of TO and LO modes, as shown in below

$$\epsilon_m(\omega) = \epsilon_\infty \prod_j \frac{\omega_{LO_j}^2 - \omega^2 - i\gamma_{LO_j}\omega}{\omega_{TO_j}^2 - \omega^2 - i\gamma_{TO_j}\omega} \tag{1.15}$$

Where ω_{jLO} and γ_{jLO} are the resonance frequency and the damping constant of the j th LO mode, respectively. This model assumed $\gamma_{LO_j} \neq \gamma_{TO_j}$ and can used for analysis of lattice vibration of . In our case the j equal to 1, thus the formula can be rewritten as

$$\epsilon_{mr}(\omega) = \frac{\epsilon_\infty (\omega_{TO}^2 \omega_{LO}^2 - \omega_{LO}^2 \omega^2 - \omega_{TO}^2 \omega^2 + \omega^4)}{(\omega_{TO}^2 - \omega^2)^2 + \gamma_{TO}^2 \omega^2} \tag{1.16}$$

$$\epsilon_{mr}(\omega) = \frac{\epsilon_\infty (\omega^3 \gamma_{TO} + \omega_{TO}^2 \gamma_{LO} \omega - \omega_{LO}^2 \gamma_{TO} \omega - \omega^3 \gamma_{LO})}{(\omega_{TO}^2 - \omega^2)^2 + \gamma_{TO}^2 \omega^2} \tag{1.17}$$

III. Results and Discussion

The constant value of the ablation threshold for femtosecond laser pulse is basically due to the fact that thermal penetration depth $l = k_e \tau_a^{1/2}$ is smaller than optical penetration depth δ where k_e is the thermal conductivity and τ_a is the ablation time. In this case threshold fluence F_{th} could be written as $F_{th} \parallel \rho \Omega \delta = I(z,t)t$, where ρ is the density, Ω is the specific heat of evaporation. The optical penetration depth δ can be expressed as

$\delta = \frac{c}{\omega \text{Im} [\epsilon(t, x, \omega)]}$, where $\text{Im} [\epsilon(t, x, \omega)]$ is the imaginary part of the refractive index. The optical

penetration depth does not rely on pulse duration, so the threshold fluences are approximately the same for different pulse durations. The behavior of threshold fluence varies as the square root of the laser pulse duration τ_L larger than 1 ps results from the threshold for ablation being controlled primarily by the thermal diffusion of the incident laser pulse energy. In this situation the heat penetration depth is much larger than the optical penetration depth and threshold fluence can be written as

$F_{th} \parallel \rho \Omega k_e \tau_a^{1/2} \exp \left(- (2 \ln 2)^2 \frac{(t - 2\tau_e)^2}{\tau_L^2} \right) \exp \left(\frac{\Delta z}{\delta} \right)$ which is in direct proportion to $\tau_a^{1/2}$. Note that in

this case, $\tau_L \gg \tau_i$, the ablation time $\tau_a = \frac{\tau_e \tau_L}{\tau_e + \tau_L}$ where τ_e and τ_L are the electron cooling and the lattice heating

times, so threshold fluence varies as $\tau_L^{1/2}$, which is understandable. Solving the first three above equations, assuming a rectangular temporal profile of the laser pulse of intensity I_0 and duration τ_L , results in an approximate expression for the attainable lattice temperature:

$$T_i(t) \parallel \frac{I(z).t}{C_i} \frac{1}{l^2 - \delta^2} \left[l \exp \left(- \frac{z}{l} \right) - \delta \exp \left(- \frac{z}{\delta} \right) \right] \tag{1.18}$$

Where F_{th} is the absorbed fluence, $\delta = 1/\alpha$ is the optical penetration depth, and l is the electron heat diffusion length given by the absorption coefficient of plasma can be estimated to $a \approx \frac{\gamma \omega^2}{\omega^2 c} \parallel \frac{N_e N_p}{\omega^2} \parallel \lambda^2$.

Consequently, irradiation of metals with laser radiation at $\lambda = 800$ nm results in a critical electron density: $N_c \approx 1.7 \times 10^{21} \text{cm}^{-3}$. Therefore, the electron-electron collisions, the diffusion of electrons out of the vapor/plasma phase, and the strong non-equilibrium conditions have to be taken into consideration for the estimation of the absorption coefficient. For the investigation of the results, high intensity laser wave interaction with semiconductor like BaTiO₃. During interaction, it induces the plasma within semiconductor materials and starts to propagate the acoustic wave. For the investigation of the results, high intensity laser wave interaction with semiconductor like BaTiO₃. During interaction, it induces the plasma within semiconductor materials and starts

to propagate the acoustic wave. As a typical case, the numerical calculation was performed for the cubic crystals at 300K, with following typical constant are taken: $n_0 = 10^{23} m^{-3}$, $m = 0.045m_0$, $\epsilon = 2000$,

$$\rho = 4.0 \times 10^3 \text{ kg / m}^3, \quad V_t = (C_{44} / \rho)^{1/2} = 2.5 \times 10^3 \text{ m / s}, \quad \Omega_p = \left(\frac{N_0 e^2}{m \epsilon_0 \epsilon_L} \right)^{1/2}, \quad K^2 = \frac{e_{14}^2}{\epsilon_L C_{44}}$$

$$c = (\mu_0 \epsilon_0 \epsilon_L)^{-1/2}, \gamma = 1 - (V_t / V_{th}) \quad v_{e-e} = 5 \times 10^{-6} N_0 \exp \left[- \frac{\Delta E}{k_B T} \right] \cdot \frac{\ln \Lambda}{T_{eV}^{3/2}}.$$

The crystal is subjected to irradiate with 10.6 μm nanosecond laser. The beauty of is that its crystal structure is easily modified by the addition of impurities or creating the defect in the lattice structure. It's easy tendency due to the formation of the solid solution with foreign atoms of the same size or fitted in the octahedral hole of the lattice arrangement. The electric field amplitude which is considered in the present investigation can be directly calculated from the

pump intensity I_0 , expressed by the following expression:
$$\frac{I_+}{I_0} = \frac{c \epsilon_0 \epsilon_L}{2\eta} \left| \frac{E_+}{E_0} \right|^2$$

(a) Calculation of modulation in $k_s > 2k$

The solid curve of Figure 1.1 represents the intensity profile with the high dielectric material. The width of the profile increases with an increase the cyclotron frequency and then suddenly decreases at the resonance frequency and beyond the cyclotron frequency it starts again increases. But at the resonance frequency, it shows the nonlinear bridge. It may be, it is due to change mode of interaction. At this point it shows the crossover for changing the E_+ modes into E_- . In Figure 1.1, the propagation of intensity or energy starts to expand with magnetic field and shows the small resonance area at which it shows the linear variation of intensity without affecting the term of $\exp(\omega_c t)$. In Figure 1.2 A & B, the change in temperature profile are plotted with the variation of cyclotron frequency. These results are plotted at two different times of interaction, i.e., at 100 and 400 fs. The profiles are similar to Figure 1.1. In Figure 1.2 A, the expansion starts from the lower frequency up to the resonance frequency, but beyond that it again shows the expanding nature. But at the resonance frequency, it shows the dropping profile for temperature. The same profile is obtained at 400 fs, time of interaction, but at this level the maximum energy is transported within the material. This shows a maximum rise in the temperature of the sample, as shown in Figure 1.2 B. Therefore, it gives the enhanced modulation in both the modes. Figure 1.3 A & B shows the variation of the temperature at the different point of interaction. This point of interaction is taken with respect to the initial point at which the first tracing of temperature profile is to be started. For the calculation of temperature profile, the value of z is taken to be 38 nm from the origin.

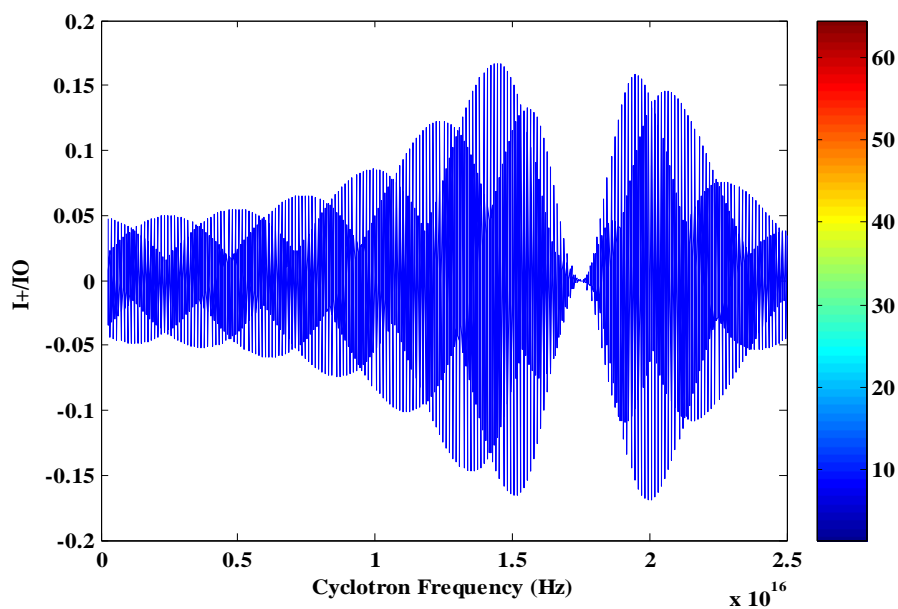
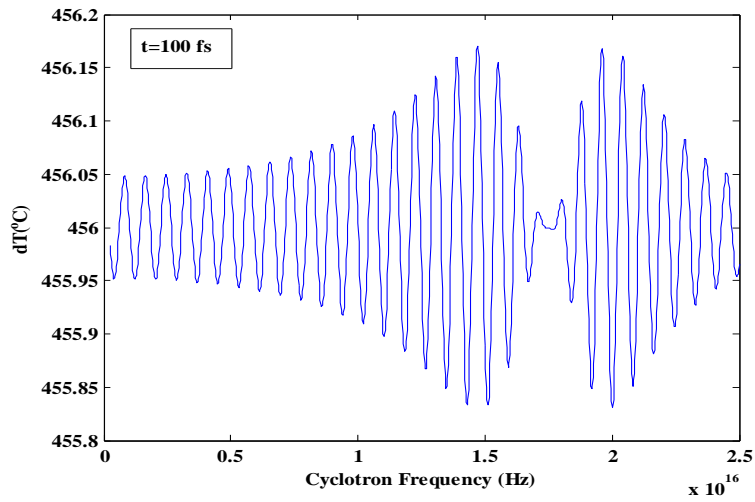
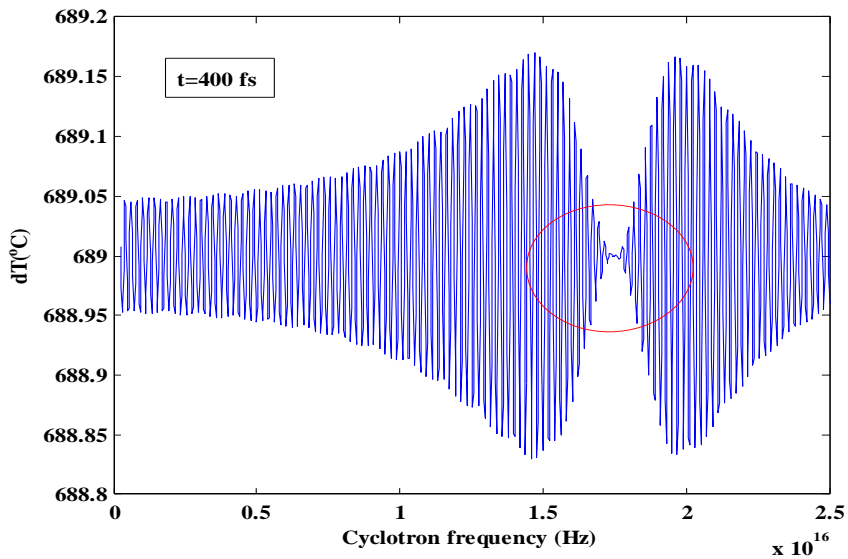


Figure 1.1: Intensity profile within, high dielectric materials.

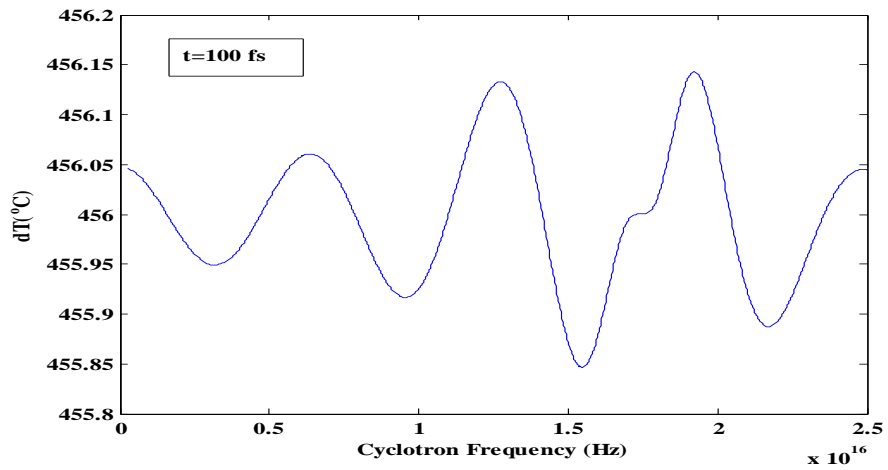


(A)



(B)

Figure 1. 2: The temperature profile with the cyclotron frequency at two different time of interaction (A) 100 (B) 400 fs



(A)

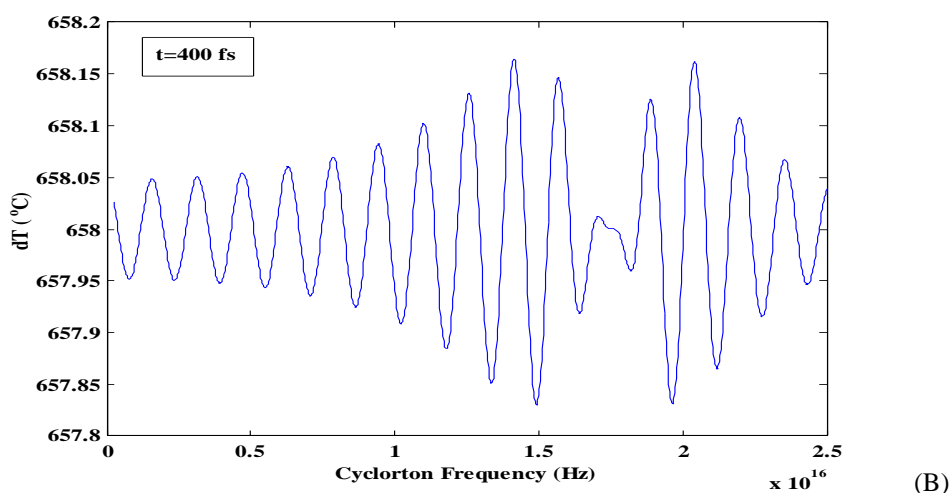
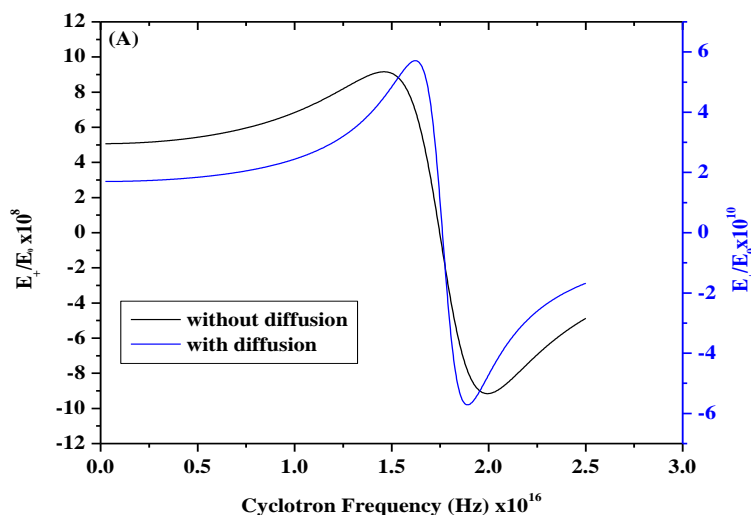


Figure 1.3: temperature profile at 38 nm from the origine with respect to cyclotron frequency.

In Figure 1.3 A, the temperature profile is completely irregular at 100 fs interaction time, but the profile is completely changed at 400 fs and followed the same feature as like intensity profile as shown in Figure 1.3 B. Hence, from the Eq (6.11), it is found that the amplitude modulations in this wave number regime are always negative. Therefore the amplitude modulations of the both the sides modes (E_{\pm}) are always out of phase with the pump wave in the permissible limit of cyclotron frequency. However the complete absorption of the wave takes place when the carrier frequency becomes equal to the pump frequency by neglecting the collision frequency. These out of phase sides bands are strongly interacting with the pump wave and induce the plasma inside the materials which demodulate the acoustic wave. Theses demodulation index is found to be maximum at a particular value of cyclotron frequency $\omega_c \approx \omega_0$. Figure 1.4 A & B in $k_s > 2k$ shows the modulation of the electric field irradiated with high intensity pump waves in both the modes, i.e., positive and negative indices with applied magneto-static field (ω_c). It is evident from the Figure 1.4 A & B that the demodulation indices on both sides first increase with cyclotron frequency up to 1.455×10^{16} Hz for and then starts to decrease up to 1.98×10^{16} Hz and again increase with an increase the cyclotron frequency. The maximum and minimum of the amplitude modulation and demodulation occurs around $E=0$, which develops the envelope around the resonance frequency. The high intensity laser beam when interact with the material then develops the heat, which modifies the modulation and demodulation process. The modulation and demodulation process is enhanced by the diffusion of the carrier heating. Figure 1.4 A & B shows the modulation and demodulation of the both the modes with the cyclotron frequency. It can also be seen from the curve that the demodulation effect of the both the modes is effectively enhanced by the incorporation of carrier heating of the material which drastically modifies the diffusion processes.



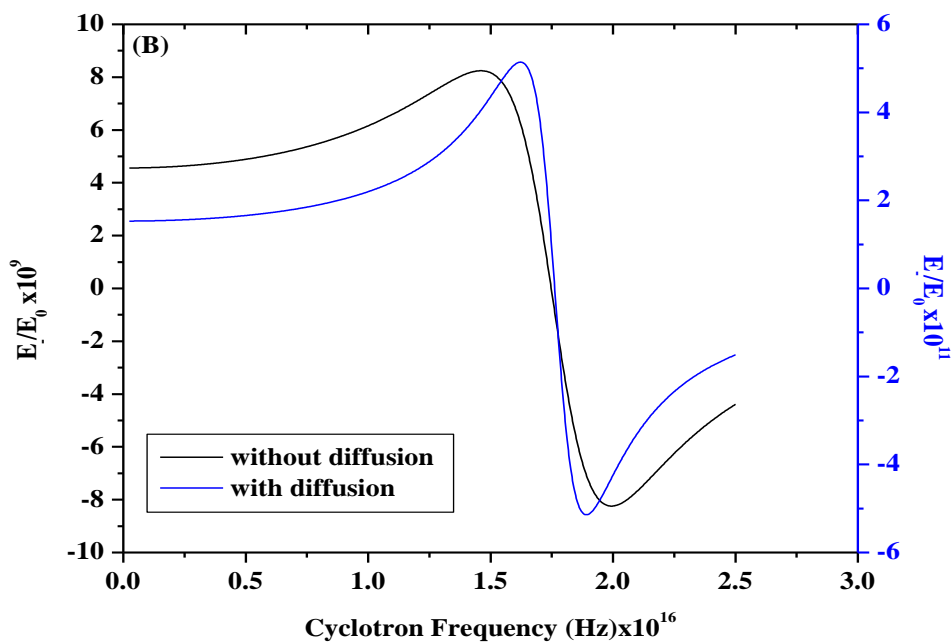


Figure 1.4: variation of modulation of (A) plus (B) negative mode (when $k_s > 2k$) with cyclotron frequency

Therefore, it gives the enhanced modulation in both the modes, as shown in Figure 1.4 A & B. The maximum and minimum turning frequency is not changed from the carrier heating and maintained the same envelope with enhanced magnitude.

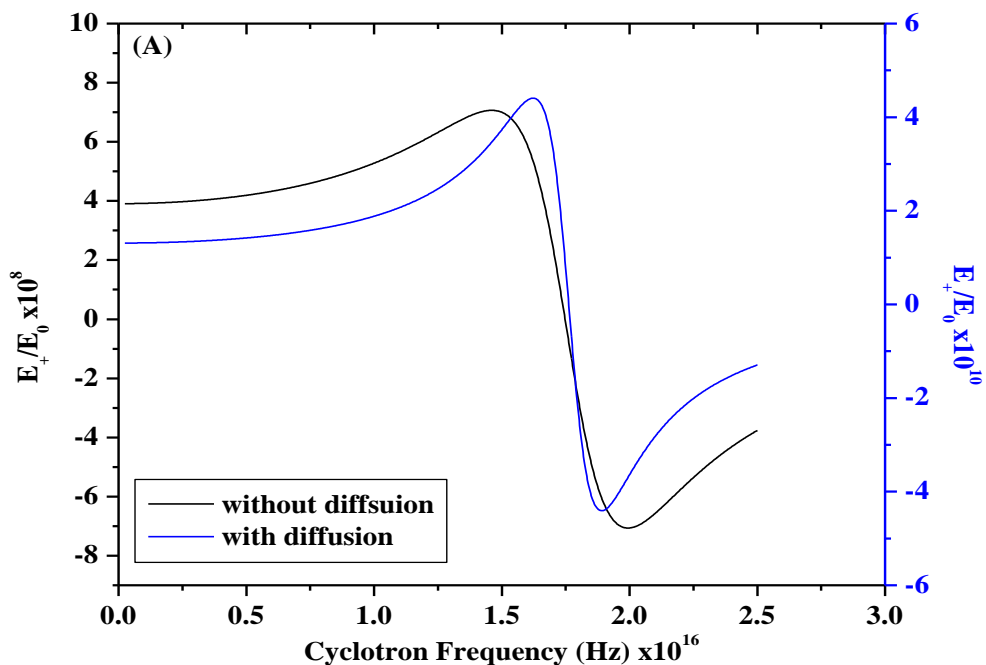
(b) Calculation of modulation in $k_s < 2k$

The same numerical investigation has been carried out in the same wave number with the following inequalities taken: $k_s < 2k$. The numerical results in this wave number regime are presented in Figure 1.5 A & B. It may be inferred from this figure that the amplitude of plus mode is out of phase with pump wave and shows the demodulation behavior and Figure 1.5 B shows the opposite behavior of the amplitude modulation of minus side mode and hence it shows the in phase with pump wave. It can be seen from these figure that a modulation index for E_+ increases with an increase the cyclotron frequency and shows the maximum at the cyclotron frequency and then it starts to decrease, while E_- decreases with an increase the cyclotron frequency and shown the minimum at the resonance frequency after that it starts to increase with cyclotron frequency. Therefore, it predicts the modulation in phase in high intense laser waves. In Figure 1.5 B, the magnitude of the demodulation process is found to be maximum at $\omega_c \approx \omega_0$. The profiles are almost same, but show only the enhancement of indices height with change the modes from positive to negative. The CH effects always increase the modulation/ and demodulation process and their effect is shown in Figure 1.5 A & B.

(c) Calculation of intensity and temperature profile in $k_s > 2k$

The intensity profile is the important profile to investigate the propagation of the high intensity laser light insides the high dielectric material. The profile depends upon the modulation and demodulation of the electric field and the cyclotron frequency. Figure 1.6 shows the variation of intensity modulation of (A) plus (when $k_s > 2k$) (B) negative mode (when $k_s < 2k$) with cyclotron frequency. The absorption depends upon the variation of intensity and the angle of interaction of wave with rotating BaTiO₃ semiconductor and slowly decreases with further increase the laser fluence. At any arbitrary angle θ , the parametric decay of intensity ratio is significantly modified from the semiconductor plasma, induced by the opto-acoustic interaction. This is relevant for the better application of laser-plasma interaction with opto-acoustic wave. Figure 6.6 shows the variation of the $I+/I_0$ with cyclotron frequency in two extreme conditions, i.e., (a) without diffusion and (b) with diffusion of charge carrier. The decay instability of intensity from the modulation and demodulation in an

isotropic and longitudinally-magnetized plasma is arising from slightly induced the nonlinear current with the application of applied voltage and the interaction from the pump wave with the acoustic phonon vibration and scattered electromagnetic wave. That's why; it reduces the intensity ratio at the resonance frequency. The absorbed power during the propagation of the acoustic wave inside, the material is directly proportional to the intensity of the laser wave and the electric conductivity of the target material used in the experiment. The electric field ratio either in modulation or demodulation with $k_s > 2k$ decreases monotonically inside the target material, whereas the electric field in $k_s < 2k$ conduction, decreases in positive mode and increases monotonically in negative modes with the cyclotron frequency inside the target material. The conductivity of the target material is very sensitive to the temperature profile and the absorbance of the power takes place above the Fermi-temperature and their profile follow the nontrivial shape. The electron-electron collision frequency is also changed with changing the conductivity of the target material according to the temperature dependent profile. Electron heat flux plays the important role when the target material is heated with the laser source. At this instant time, the laser wave is completely absorbed by the target material with enhanced magnitude. Figure 1.7 shows the intensity profile at the different temperature. The target material is heated from 100 to 700°C, and only changed the electron-electron collision frequency, which is responsible for changing the magnitude of the intensity ratio. The other responsibility factor is the diffusion, which changed from the change in temperature profile. The CH effect is more dominant at the higher temperature with enhanced magnitude. The other important effect is angle of interaction of incident wave with the target material. Figure 1.8 shows the interaction of wave at a 120° angle of incidence. In this study, it is found that the profile of the intensity varies negative with cyclotron frequency. In this view, the electric field modulation in $k_s > 2k$ increases monotonically with the cyclotron frequency and energy growth occurs opposite to heat flux from the interaction with laser wave. The intensity profile in diffusion is reduced because of the heat flux developing from the movement of the electron in the opposite direction of the electric field modulation and demodulation. The field modulation or demodulation actually changes the movement of the electron-electron collision. From this reason It may be the inverted the profile of intensity in the opposite direction.



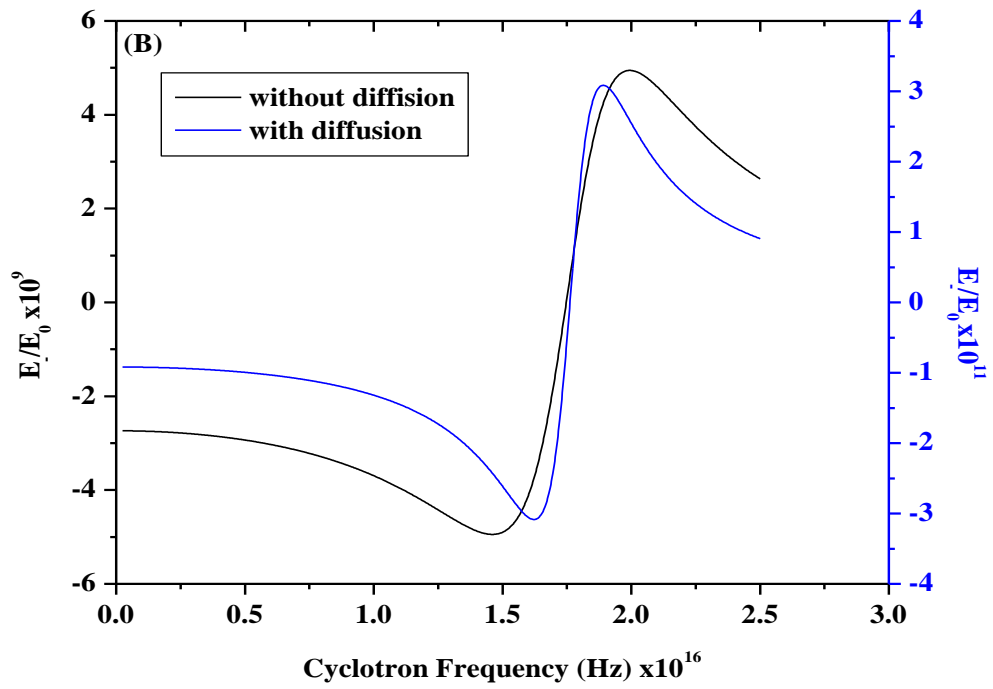
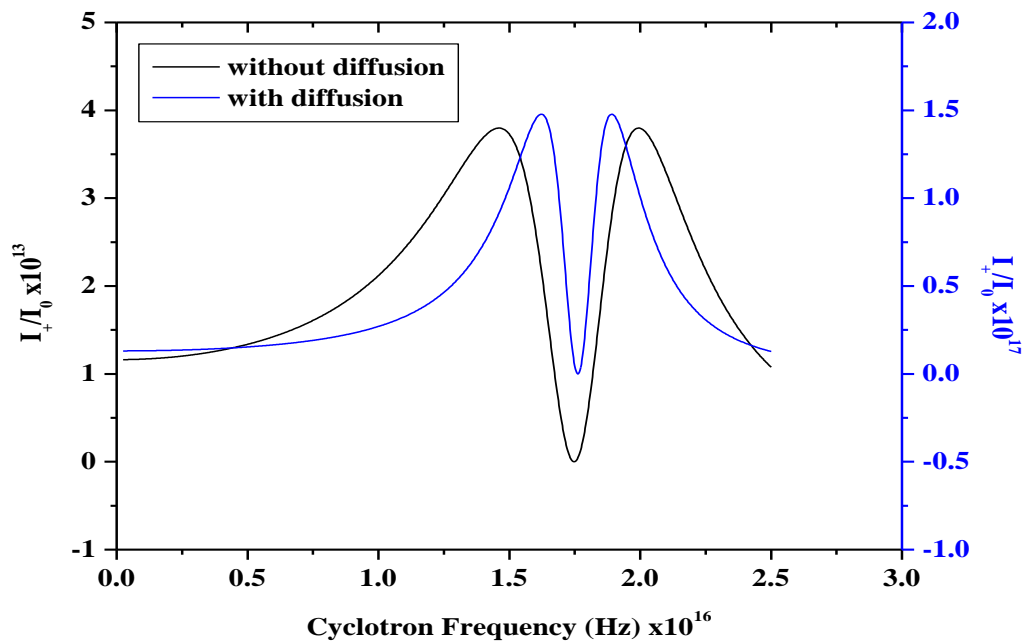


Figure 1.5: variation of modulation of (A) plus (B) negative mode (when $k_s < 2k$) with cyclotron frequency



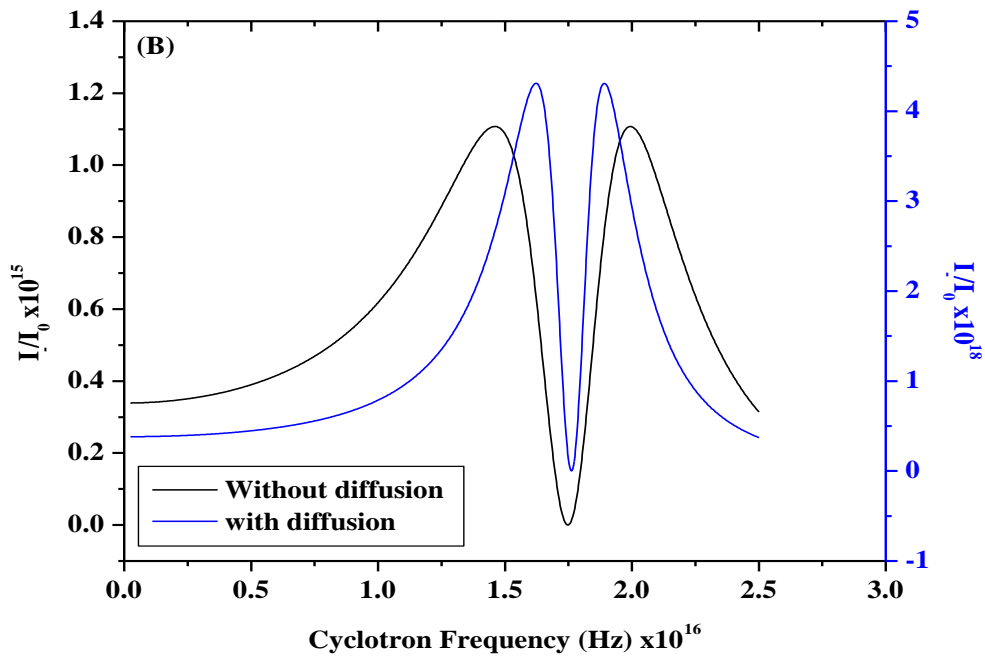


Figure 1.6: variation of intensity modulation of (A) plus (when $k_s > 2k$) (B) negative mode (when $k_s < 2k$) with cyclotron frequency

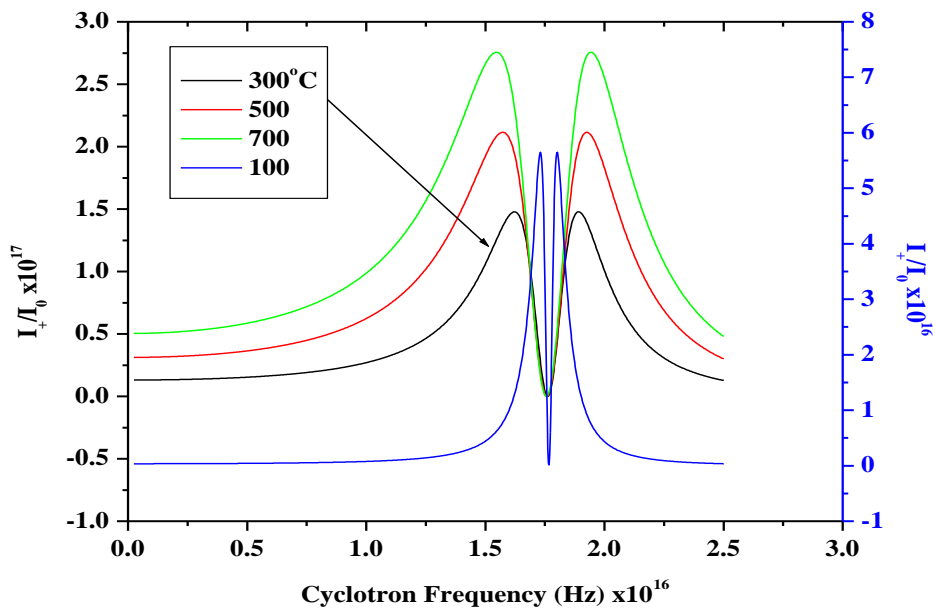


Figure 1.7: variation of intensity modulation of plus (when $k_s > 2k$) with cyclotron frequency at the different operating temperature

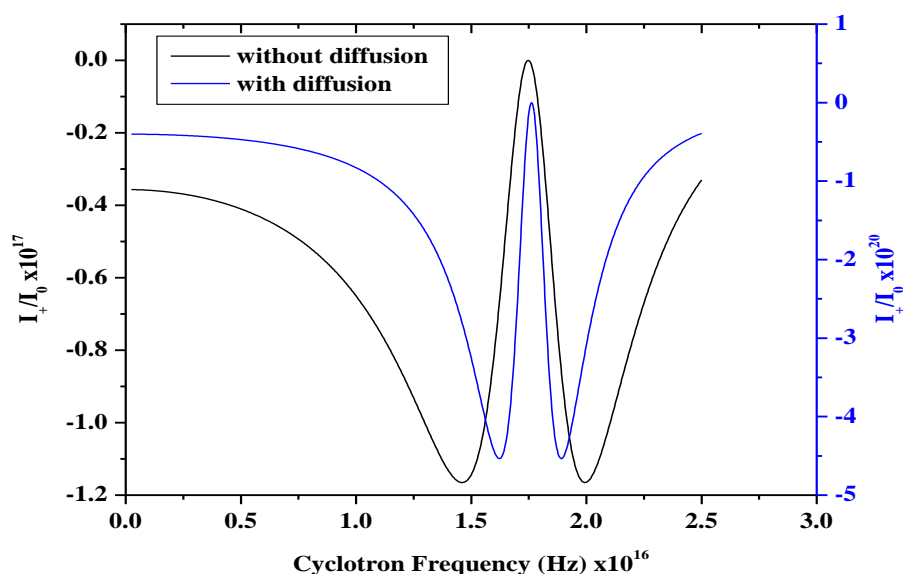


Figure 1.8: variation of intensity modulation of plus (when $k_s > 2k$) with cyclotron frequency at the different 300°C, but pump waves interact with at 120° angle of incident.

IV. Conclusion

The above study reveals that the complete absorption takes place in wide regions of the magnetic field depending upon the modulation and demodulation of the intensity either in positive and negative modes. The intensity and temperature profile starts to expand from the lower to higher cyclotron frequency. The amplitude modulation and demodulation decreases monotonically with an increase the cyclotron frequency and their intensity variation in both the modes take place around the resonance frequency ω_0 . While the opposite trends are observed in $ks < 2k$ with negative indices. At the resonance frequency, the modulation and demodulation try to approach the zero value. The CH effect always shows the enhanced modulation and demodulation indices for both the modes through temperature dependent diffusion processes. The negative intensity profile with decrease the effect of CH are observed in back sides interaction of the laser wave. Their effect also opened the new approach in strain dependent high dielectric material with acousto-optic polarization for the designing of energy transmission and temperature measurement device for diagnostic ultra-short laser high intensity laser wave.

Acknowledgement- The authors are very much thankful to Principal Govt. M.V.M College and Material Science & Metallurgical Engineering Department MANIT for providing facilities.

References

- [1]. T. H. Maiman, "Stimulated optical radiation in ruby," Nature, vol. 187, no. 4736, pp. 493–494, (1960)
- [2]. J. A. Armstrong, N. Bloembergen, J. Ducuing, and P. S. Pershan, "Interactions between light waves in a nonlinear dielectric," Physical Review, vol. 127, no. 6, pp. 1918–, (1962)
- [3]. N. Bloembergen and P. S. Pershan, "Light waves at boundary of nonlinear media," Physical Review, vol. 128, no. 2, pp. 606–(1962)
- [4]. N. Bloembergen, "Wave propagation in nonlinear electromagnetic media," Proceedings of the Ieee, vol. 51, no. 1, pp. 124 (1963)
- [5]. Lan Jiang, , Hai-Lung Tsai "Modeling of ultrashort laser pulse-train processing of metal thin films" International Journal of Heat and Mass Transfer 50 ,3461–3470 (2007)
- [6]. K. Sokolowski-Tinten, J. Bialkowski, A. Cavalleri, M. Boing, H. Sch" uler, and D. von der Linde, "Dynamics of femtosecond laser induced ablation from solid surfaces," in High Power Laser Ablation, C. R. Phipps, ed., Proc. SPIE3343, pp. 46–57, 1998.
- [7]. K. Sokolowski-Tinten, J. Bialkowski, A. Cavalleri, D. von der Linde, A. Oparin, J. Meyer-ter-Vehn, and S. I. Anisimov, "Transient states of matter during short pulse laser ablation," Phys. Rev. Lett. 81, pp. 224–227 (1998)
- [8]. G. I. Stegeman and M. Segev, "Optical Spatial Solitons and their interactions" Science 286, 1518 (1999).
- [9]. H. Schroeder and S. L. Chin "Visulization of the evolution of multiple filament in methanol" Optics Communications 234, 399 (2004).
- [10]. T. Apostolova "Theoretical study of sub-to-picosecond laser pulse interaction with dielectrics, semiconductors and semiconductor heterostructures " Journal of Physics: Conference Series 113 , 012045 IOP Pub. (2008)
- [11]. F. Rossi and T. Kuhn "Theory of ultrafast Phenomena in Photoexcited Semiconductors" Rev. Mod. Phy. 74, 895 (2002)
- [12]. S.K. Sundaram and E. Mazur "Inducing and probing non-thermal transitions in semiconductors using femtosecond laser pulses" Nature materials 1 , 217(2002)

- [13]. J. R. Davies “ Laser absorption by overdense plasmas in the relativistic regime ” Plasma Phys. and Control Fusion 51, 014006 (2009)
- [14]. Y. Ping et al. “ Absorption of short laser pulses on solid targets in the ultrarelativistic regime ”Phys. Rev. Lett. 100, 085004 (2008)
- [15]. J. P. Geindre , R.S. Marjoribanks, P. Audebert “ Electron vacuum acceleration in a regime beyond Brunel absorption” Phys. Rev. Lett. 104, 135001 (2010)
- [16]. J. P. Gordon “Interaction forces among Solitons in optical fibers ”Optics Letters **8**, 596 (1983).
- [17]. S.Kato , R Kawakami , K. Mima “Nonlinear Inverse Bremsstrahlung in Solid Density Plasmas” Phys. Rev. A. 43(10): 5560-5567.(1991)
- [18]. Wang X.Y., Downer M.C. “Femtosecond Time-Resolved Reflectivity of Hydrodynamically Expanding Metal Surfaces”Optics Letters. 17(20): 1450-1452 (1992)
- [19]. Rethfeld B., Kaiser A., Vicanek M., Simonc G. “Nonequilibrium Electron and Phonon Dynamics in Solids Absorbing a Subpicosecond Laser Pulse” Proc. SPIE. 4423: 250-261.(2001)
- [20]. B. Rethfeld , A.Kaiser., M. Vicanek , G. Simon “Ultrafast Dynamics of Nonequilibrium Electrons in Metals under Femtosecond Laser Irradiation.” Phys. Rev. B. 65: 214303-214313(2002)
- [21]. Ashcroft N.W., Mermin N.D. “Solid State Physics. New York: Holt, Rinehart, and Winston. 826 (1976).
- [22]. R. Stoian “Investigation of the Dynamics of Material Removal in Ultrashort Pulsed Laser Ablation of Dielectrics ” Freie Universität Berlin (2000)

IOSR Journal of Applied Physics (IOSR-JAP) (IOSR-JAP) is UGC approved Journal with SI. No. 5010, Journal no. 49054.

Shivani saxena "Study of Absorption from Intensity Modulation and Demodulation of an Ultra-Short Pulse Laser in High Magnetic Field from Acousto-Optic Strain Dependent High Dielectric Constant Diffusive Ferroelectric Semiconductor Plasma." IOSR Journal of Applied Physics (IOSR-JAP) , vol. 9, no. 6, 2017, pp. 58-71.